Am J Physiol Cell Physiol 299: C614–C620, 2010.
First published May 12, 2010; doi:10.1152/ajpcell.00074.2010.

On the substrate recognition and negative regulation of SPAK, a kinase modulating Na^+-K^+-$2Cl^-$ cotransport activity

Kenneth B. Gagnon and Eric Delpire

Department of Anesthesiology, Vanderbilt University School of Medicine , Nashville, Tennessee

Submitted 8 March 2010; accepted in final form 7 May 2010

Gagnon KB, Delpire E. On the substrate recognition and negative regulation of SPAK, a kinase modulating Na^+-K^+-$2Cl^-$ cotransport activity. *Am J Physiol Cell Physiol* 299: C614–C620, 2010. First published May 12, 2010; doi:10.1152/ajpcell.00074.2010.—Threonines targeted by Ste20-related proline-alanine-rich kinase (SPAK) for phosphorylation have been identified in Na^+-K^+-$2Cl^-$ cotransporter type 1 (NKCC1), NKCC2, and Na^+-Cl^- cotransporter (NCC). However, what constitutes the substrate recognition of the kinase is still unknown. Using site-directed mutagenesis and functional measurement of NKCC1 activity in *Xenopus laevis* oocytes, we determined that SPAK recognizes two threonine residues separated by four amino acids. Addition or removal of a single residue abrogated SPAK activation of NKCC1. Although both threonines are followed by hydrophobic residues, in vivo experiments have determined that SPAK activation of the cotransporter only requires a hydrophobic residue after the first threonine. Interestingly, downstream of the second threonine residue, we have identified a conserved aspartic acid residue which is critical for NKCC1 function. Mouse SPAK activity requires phosphorylation of two specific residues by WNK [with no lysine (K)] kinases: a threonine (T243) in the catalytic domain and a serine (S383) in the regulatory domain. We found that mutating the threonine residue into a glutamic acid (T243E) combined with mutation of the serine into an aspartic acid (S383D) rendered SPAK constitutively active. Surprisingly, alanine substitution of S383 or mutation of residues surrounding this residue also resulted in a constitutively active kinase. Interestingly, deletion of amino acids 356–398 identified another serine residue in the catalytic domain (S321) as another putative target of WNK phosphorylation. We found that WNK4 is capable of stimulating the deletion mutant when S321 is present, but not when S321 is mutated into an alanine.

NKCC1; WNK kinase; constitutive activity; *Xenopus* oocytes; Ste20-related proline-alanine-rich kinase

COUPLED ELECTRONEUTRAL MOVEMENT of Na^+, K^+, and Cl^- is mediated by two Na-K-2Cl cotransporter mechanisms, NKCC1 and NKCC2. NKCC2 is exclusively expressed in the thick ascending limb of Henle and macula densa cells of the kidney where it participates in the reabsorption of salt and water (2, 18). NKCC1 is more widely expressed and serves diverse functions in the body, such as Cl^- secretion in a variety of epithelia (22), K^+ secretion in the inner ear (5, 9), and modulation of GABA neurotransmission in sensory neurons (1, 30).

These two cotransporters are activated by phosphorylation of specific threonine residues located in their cytosolic NH_2-terminal domain (6, 16, 32). Work from this laboratory and others has shown that Ste20-related proline-alanine-rich kinase (SPAK) and oxidative stress response kinase 1 (OSR1), two mammalian Ste20p-like kinases, physically interact with the cytosolic NH_2-terminal domain of the cotransporter (28, 32). Whether cotransporter phosphorylation is solely due to SPAK and OSR1 or is also due to additional, as yet unidentified, kinases is still unresolved. Interaction occurs between a structured and highly conserved domain of the regulatory COOH terminus of the kinase and a nine-residue peptide containing the core consensus sequence RFx[V/I] (28, 31). This consensus sequence is found in many proteins of the mouse proteome (8), including proteins that have been shown to physically interact with the Ste20 kinase (27).

In NKCC1, binding of the kinase occurs at two locations, some 70 and 130 residues upstream of the phosphorylation site. Experiments performed in vitro as well as in vivo have shown that binding of SPAK is a prerequisite to phosphorylation and activation of the cotransporter (14). Although essential, substrate binding is not the only determinant of kinase specificity. Protein kinases phosphorylate their targets at discrete sites, and these targeting sites are typically defined by their interaction with the activation segment of the kinase. Biochemical experiments have shown that residues T197, T201, and T206 are sites of SPAK phosphorylation (14, 32). Although not identified as a target of SPAK phosphorylation, additional experiments have indicated that phosphorylation of T211 is important for NKCC1 function (6). What in this region constitutes the determinant of SPAK recognition for substrate specificity is still unknown. In this study, using site-directed mutagenesis, we found that it is critical for the two main sites of NKCC1 phosphorylation (T206 and T211) to be separated by four amino acid residues for SPAK target recognition. We have identified a hydrophobic residue immediately following threonine 206 (F207) and a negatively charged residue two residues downstream of threonine 211 (D213) which are critical for kinase-substrate interaction and cotransporter activation. We have identified another phospho-residue (S321) critical for SPAK function. Finally, we have identified a region of the regulatory domain of SPAK that negatively regulates kinase activity.

MATERIALS AND METHODS

Site-directed mutagenesis and deletion mutants. All experiments were performed using cDNAs encoding the mouse NKCC1 (10), mouse SPAK (28), and mouse WNK4 [with no lysine (K)] (15) proteins. Single point mutations within the cytosolic NH_2-terminal domain of NKCC1 and within the kinase or regulatory domains of SPAK were performed using the QuikChange II site-directed Mutagenesis kit [Agilent Technologies (Stratagene), La Jolla, CA]. Typically, small fragments of the cotransporter or kinases were first subcloned into a pBSK engineered to include unique restrictions sites. Using complementary sense and antisense oligonucleotides, we then mutated specific residues using QuikChange II. After the synthesis reaction, the parental DNA was digested with *Dpn*I and the synthesized DNA was transformed into *Escherichia coli*. The mutated DNA was sequenced between the two restrictions sites and the fragment

Address for reprint requests and other correspondence: E. Delpire, Dept. of Anesthesiology, Vanderbilt Univ. Medical Center, T-4202 MCN 1161 21st Ave. South, Nasvhille, TN 37232-2520 (e-mail: eric.delpire@vanderbilt.edu).

returned into the original clone. For deletion of large fragments, we used sequential PCR reactions. Briefly, two PCR reactions were independently set to amplify the upstream and downstream regions of the fragment targeted for deletion. The reverse primer of the first reaction and the forward primer of the second reaction contained complementary sequences at their 5′-ends; thus, through a third PCR reaction using the forward primer of the first reaction and the reverse primer of the second reaction, we linked the two fragments together.

cRNA transcription. For expression in *Xenopus laevis* oocytes, the cDNAs or their mutants were inserted into pBF, an amphibian expression vector. Each clone was grown in Luria-Bertani broth (LB) with 0.1 mg/ml ampicillin, and the DNA was purified using a plasmid midiprep kit (Qiagen, Valencia, CA) and quantitated by measuring DNA absorbance at 260 nm. DNA (20 μg) was linearized overnight with *Mlu*I and purified using a QIAquick PCR purification kit (Qiagen). Linearized DNA (2.5 μg) was then transcribed into cRNA using Ambion's mMESSAGE mMACHINE SP6 transcription system (Ambion, Austin, TX). cRNA quality was verified by gel electrophoresis (1% agarose-0.693% formaldehyde) and quantitated by measurement of absorbance at 260 nm.

Isolation of Xenopus laevis oocytes. Stages V–VI *Xenopus laevis* oocytes were isolated from eight different frogs as previously described (15) and maintained at 16°C in modified L15 medium (Leibovitz's L15 solution diluted with water to a final osmolarity of 195–200 mosM and supplemented with 10 mM HEPES and 44 μg gentamicin sulfate). Oocytes were injected 1 day postisolation (*day 2*) with 50 nl water containing 15 ng NKCC1 cRNA and on *day 3* with 50 nl water containing 10 ng of kinase cRNA. K^+ uptake measurements were performed using ^{86}Rb as a tracer on *day 5* postisolation. All animal procedures and experiments were approved by the Vanderbilt University Institutional Animal Care and Use Committee.

K^+ uptake in Xenopus laevis oocytes. Groups of 20 oocytes in a 35-mm dish were washed once with 3 ml isosmotic saline (96 mM NaCl, 4 mM KCl, 2 mM $CaCl_2$, 1 mM $MgCl_2$, 5 mM HEPES buffered to pH 7.4, osmolarity, 200 mosM) and preincubated for 15 min in 1 ml same isosmotic saline containing 1 mM ouabain. The solution was then aspirated and replaced with 1 ml isosmotic flux solution containing 5 μCi ^{86}Rb. Two 5-μl aliquots of flux solution were sampled at the beginning of each ^{86}Rb uptake period and used as standards. After 1 h uptake, the radioactive solution was aspirated and the oocytes were washed four times with 3 ml ice-cold isosmotic solution. Hyperosmotic saline (265 mosM) was obtained by adding 65 mM sucrose to the isosmotic saline. Single oocytes were transferred into glass vials, lysed for 1 h with 200 μl 0.25 N NaOH, and neutralized with 100 μl glacial acetic acid, and ^{86}Rb tracer activity was measured by β-scintillation counting. NKCC1 flux is expressed in nanomoles K^+ per oocyte per hour.

Surface expression of NKCC1 in Xenopus laevis oocytes. Groups of 50 oocytes were injected on *day 2* after isolation with 50 nl water containing 18.5 ng of NKCC1 (wild-type and mutant) cRNA. On *day 5*, the oocytes were washed with isosmotic flux solution and gently rotated every 10 min on ice with 2.5 ml isotonic flux solution containing 1 mg/ml EZ-link sulfo-NHS biotin (Pierce, Thermo Fisher Scientific, Rockford, IL) for 2 h. Following the biotin labeling, oocytes were washed three times with an isotonic solution containing 100 mM glycine, then placed in 20 μl/oocyte of lysis buffer [150 mM NaCl, 10 mM Tris-Cl (pH 7.4), 1 mM EDTA, 1% Triton X-100, and protease inhibitors (Roche Applied Science, Indianapolis, IN)] on ice for 15 min. Oocytes were homogenized by trituration with a 200 μl pipette, rotated at 4°C for 1 h, then centrifuged for 15 min at 10,000 rpm. Supernatants were rotated overnight at 4°C with 75 μl streptavidin bead slurry (50% in lysate buffer). Samples were centrifuged for 2 min at 8,000 rpm, and the streptavidin beads were washed three times with lysis buffer before the addition of 4× sample buffer (0.26 M Tris, pH 6.8, 4.8% SDS, 40% glycerol, and 0.002% bromophenol blue). After 20 min denaturation at 60°C, the samples were loaded and separated on 7.5% polyacrylamide gels and transferred to polyvinylidene difluoride (PVDF) membranes (Thermo Fisher Scientific, Pittsburgh, PA). Membranes were blocked for 2 h at room temperature with 5% nonfat dry milk in TBS-T [150 mM NaCl, 10 mM Tris·HCl, 0.5% Tween 20 (polyoxyethylene-sorbitan monolaurate)], then probed with a mouse anti-NKCC1 polyclonal antibody (1:1,000) overnight at 4°C. Membranes were rinsed several times in TBS-T before a 1 h incubation with an anti-mouse horseradish peroxidase-conjugated secondary antibody (1:4,000) in 5% nonfat dry milk in TBS-T at room temperature. The membranes were again rinsed several times in TBS-T, then finally subjected to enhanced chemiluminescence (ECL) detection (Amersham Biosciences, Piscataway, NJ).

Statistical analysis. K^+ uptake was measured in individual oocytes by scintillation counting. Each experimental group was represented by 20 to 25 oocytes (n = 20–25). Differences between groups were tested using one-way ANOVA, followed by multiple comparisons using the Student-Newman-Keuls, Bonferroni, and Tukey's post hoc tests. $P > 0.05$ was considered to be nonsignificant, whereas $P < 0.001$ was considered to be very significant. Recognizing that an absence of significance between specific groups might be the result of a type II error, we conducted one-way ANOVA on a logarithmic transformation of the data. Significant results ($P < 0.001$) of these additional analyses are identified in the figures by solid horizontal lines.

RESULTS

Alignment of the Na^+-dependent cation chloride cotransporters NCC, NKCC1, and NKCC2 illustrates the location of several conserved threonine residues targeted by SPAK for phosphorylation (see Fig. 1). However, what constitutes the entire kinase substrate recognition site has not yet been fully determined. To gain insight on SPAK substrate recognition, we targeted for mutagenesis residues around the key threonines relevant to NKCC1 activation. Cotransporter activity measured through K^+($^{86}Rb^+$) uptake demonstrates that SPAK substrate recognition involves two threonines (T206 and T211) separated by four amino acids. This is based on the observation that mutagenesis of either threonine (T206A or T211V), removal of a single amino acid shortening the sequence to three residues (G208− or H209−), or insertion of a single amino acid lengthening the sequence to five residues (+A209) completely disrupted cotransporter function (Fig. 2). The imidazole sidechain of histidine has a pKa of ~6 (11), whereas the entire amino acid has a pKa of 7.6. As a result, an acidic shift in the pH will cause the imidazole ring to become protonated and positively charged. We mutated the histidine residue into an

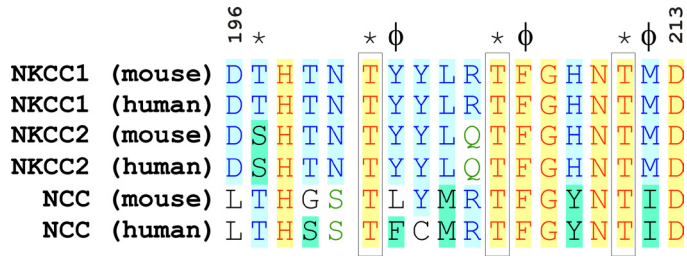

Fig. 1. Alignment of mouse and human Na^+-dependent cation chloride cotransporter sequences around the phosphothreonines. Identical residues are in red font over yellow background, while conserved residues are in black or blue fonts over green and blue backgrounds. The sites of phosphorylation are indicated with a star. Note that the residues that directly follow the threonine residues are hydrophobic (ϕ) in nature. Numbers at *top* indicate amino acid position of mouse Na-K-2Cl cotransporter type 1 (NKCC1). NCC, Na^+-Cl^- cotransporter.

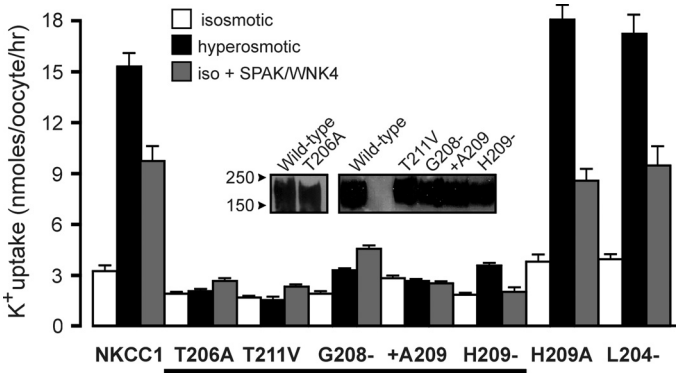

Fig. 2. Distance between T206 and T211 affects NKCC1 activity in *Xenopus laevis* oocytes. Cotransporter activity was measured through $K^+(^{86}Rb^+)$ uptake under isosmotic (white bars), isosmotic with Ste20-related proline-alanine-rich kinase (SPAK) and WNK4 [with no lysine (K)] coexpression (gray bars), or hyperosmotic (black bars) conditions. Residue numbers correspond to the mouse NKCC1 sequence. Bars represent means ± SE of the flux (expressed in nanomoles per oocyte per hour; $n = 20–25$ oocytes). Each condition was reproduced at least once with independent oocytes from different frogs. All underlined mutants were significantly ($P < 0.001$) different from control (wild-type NKCC1) K^+ uptake under their respective conditions (see MATERIALS AND METHODS). *Inset*: biotinylated NKCC1 signal obtained with different nonfunctional cotransporters, compared with wild-type NKCC1.

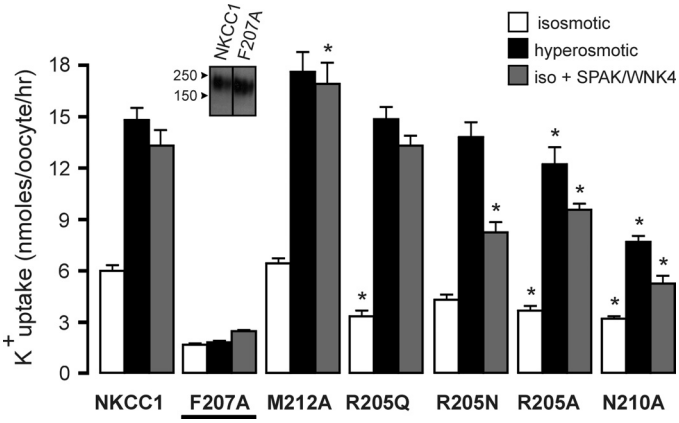

Fig. 3. Additional mutations around T206 and T211 on NKCC1 activity in *Xenopus laevis* oocytes. NKCC1 activity was measured through $K^+(^{86}Rb^+)$ uptake under isosmotic (white bars), isosmotic with SPAK and WNK4 coexpression (gray bars), or hyperosmotic (black bars) conditions. Residue numbers correspond to the mouse NKCC1 sequence. Bars represent means ± SE of the flux (expressed in nanomoles per oocyte per hour; $n = 20–25$ oocytes). Each condition was reproduced at least once with independent oocytes from different frogs. *Significant ($P < 0.001$) difference from control (wild-type NKCC1) K^+ uptake under their respective conditions. The underlined mutant was also significantly ($P < 0.001$) different from control (wild-type NKCC1) K^+ uptake under their respective conditions (see MATERIALS AND METHODS). *Inset*: biotinylated NKCC1 signal obtained with F207A cotransporter compared with wild-type NKCC1.

alanine (H209A) to determine whether the imidazole ring of H209 played a role in kinase-substrate interaction. Although deletion of the histidine residue (H209−) eliminated cotransporter activity, mutation into an alanine residue (H208A) had no functional consequence, suggesting that the imidazole sidechain of the histidine residue does not have a role in kinase-substrate interaction (Fig. 2). To eliminate the possibility that our mutagenesis studies were impeding trafficking of the cotransporter to the plasma membrane, we used biotin labeling/streptavidin bead pull-down and a NKCC1 polyclonal antibody to verify equivalent cell surface expression of wild-type and mutant forms of the cotransporter (Fig. 2, *inset*). Interestingly, there is another threonine residue four amino acids upstream of T206 which has been identified as a target of SPAK phosphorylation. However, deletion of a leucine residue (L204−) shortening the sequence between T201 and T206 to three residues had no deleterious effects on cotransporter function (Fig. 2).

As many kinases have a P + 1 hydrophobic pocket, we examined the importance of the hydrophobic residues (F207 and M212) that directly follow the two key threonines involved in SPAK substrate recognition. We found that mutation of F207 into alanine significantly impacted function, whereas mutation of M212 into alanine had no effect on function (Fig. 3). Biotinylation of *Xenopus laevis* oocytes expressing the F207A mutant form of NKCC1 confirms that trafficking to the plasma membrane was unimpeded (Fig. 3, *inset*). Protein alignments between NKCC1 and NKCC2 in different species highlighted the predominance of arginine, asparagine, and glutamine residues immediately preceding the threonines important to kinase substrate recognition. Whereas mutation of arginine into a glutamine (R205Q), into an asparagine (R205N), or into an alanine (R205A) had only minimal effect on NKCC1 function, alanine substitution of asparagine (N210) significantly reduced cotransporter function (Fig. 3). Because charged residues immediately adjacent of substrate recognition sites are often involved in forming bonds with other residues in the catalytic domain, we addressed the role of two aspartic acids flanking the phosphothreonine region. While the upstream aspartate (D196) is only conserved within the Na-K-2Cl cotransporters, the downstream aspartate (D213) is also conserved in the Na^+-Cl^- cotransporter. As seen in Fig. 4, mutation of the upstream aspartate into alanine (D196A) had no effect on NKCC1 function, whereas mutation of the downstream aspar-

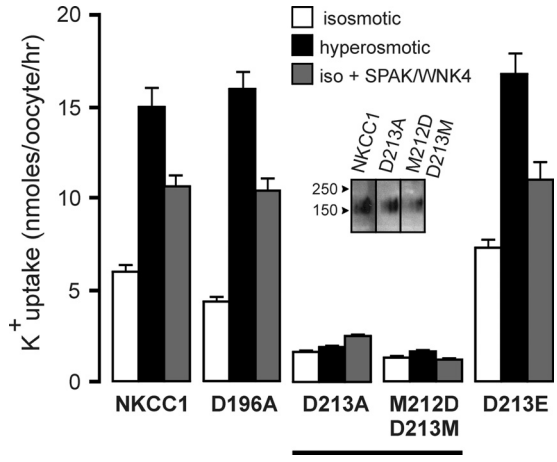

Fig. 4. Role of two conserved aspartic acids on NKCC1 activity in *Xenopus laevis* oocytes. NKCC1 function was measured through $K^+(^{86}Rb^+)$ uptake under isosmotic (white bars), isosmotic with SPAK and WNK4 coexpression (gray bars), or hyperosmotic (black bars) conditions. Residue numbers correspond to the mouse NKCC1 sequence. Bars represent means ± SE of the flux (expressed in nanomoles per oocyte per hour; $n = 20–25$ oocytes). Each condition was reproduced at least once with independent oocytes from different frogs. Underlined mutants were significantly ($P < 0.001$) different from control (wild-type NKCC1) K^+ uptake under their respective conditions (see MATERIALS AND METHODS). *Inset*: biotinylated NKCC1 signal obtained with different nonfunctional cotransporters, compared with wild-type NKCC1.

tate (D213A) abrogated NKCC1 function. Further mutagenesis demonstrated that this residue could not be moved one position up (M212D, D213M), but could be substituted by another negatively charged residue (D213E). Again, we used biotinylation and Western blot analysis to confirm that the lack of cotransporter activity was not a result of trafficking to the plasma membrane (Fig. 4, *inset*).

We have shown previously that for activation of NKCC1 in *Xenopus laevis* oocytes, both SPAK and WNK4 kinases needed to be co-injected, because SPAK alone had no effect on NKCC1 function (15). Because the catalytic activity of WNK4 and the presence of a SPAK interacting domain were necessary for this activation, we further postulated that WNK4 phosphorylates and activates SPAK prior to the kinase phosphorylating and activating NKCC1. Using mass spectrometry analysis and Edman sequencing, two groups have demonstrated that a threonine residue in the activating segment (T243) and a serine reside in the regulatory COOH terminus (S383) were targets of WNK4 phosphorylation (23, 32). However, we could not reconcile why if S383 was a critical phospho-residue, its mutation into alanine had no effect on SPAK activity. Here we show that mutation of S383 into an alanine in combination with T243E renders the kinase constitutively active, irrespective of the presence or absence of WNK4. Figure 5 shows that mutation of either of these residues singly had no effect on SPAK activity and still required the presence of WNK4 for activation. Interestingly, although phosphorylation of T243 could not be mimicked by substitution into an aspartate (data not shown), mutation of S383 into an aspartic acid (in conjunction with T243E) activated the kinase (Fig. 5).

Many kinases, including Ste20 kinases, have been shown to possess autoinhibitory domains (for review see Ref. 7). To test whether S383 was part of such a domain in SPAK, we mutated several residues upstream and downstream of S383. Interestingly, all the mutations we created and tested resulted in cotransporter activation, indicating the importance of this entire region to SPAK regulation (Fig. 6). We also deleted most of the regulatory region between the

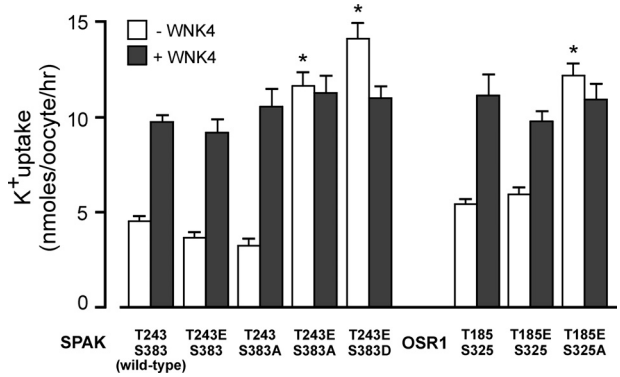

Fig. 5. Targeted mutations in SPAK and oxidative stress-responsive kinase 1 (OSR1) render the kinases constitutively active. Kinase activity was assessed in *Xenopus laevis* oocytes through its ability to activate wild-type NKCC1 in the absence (white bars) or presence (black bars) of WNK4. NKCC1 activity was measured through $K^+(^{86}Rb^+)$ uptake under isosmotic conditions. Bars represent means ± SE of the flux (expressed in nanomoles per oocyte per hour; $n = 20–25$ oocytes). Each condition was tested at least twice with independent oocytes isolated from different frogs. *Significant ($P < 0.001$) difference from control conditions (NKCC1 + wild-type SPAK or NKCC1 + wild-type SPAK + WNK4).

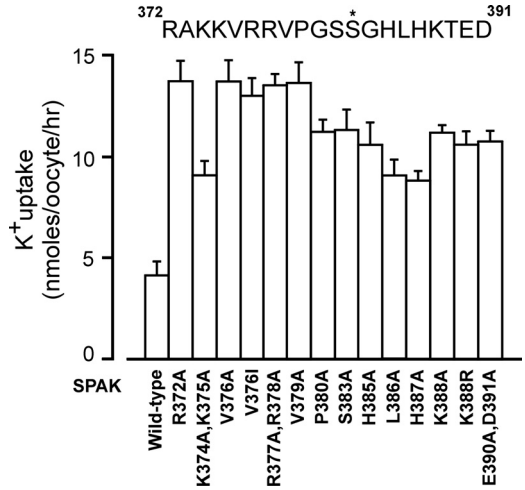

Fig. 6. Targeted mutations in the S383-containing segment activate SPAK 243E. To test for constitutive activity in the absence of WNK4, NKCC1 activity was measured through $K^+(^{86}Rb^+)$ uptake in *Xenopus laevis* oocytes coexpressing SPAK with the T243E mutation only (wild-type) or containing additional mutations in the S383 domain. All fluxes were performed under isosmotic conditions. The residues surrounding S383 and targeted for mutation are presented. S383 is denoted by an asterisk. Bars represent means ± SE of the flux (expressed in nanomoles per oocyte per hour; $n = 20–25$ oocytes). Each condition was tested at least twice with independent oocytes isolated from different frogs. All K^+ uptakes with mutant kinases were significantly ($P < 0.001$) different from K^+ uptake with wild-type kinase.

catalytic domain and the putative caspase site (DEMD). To our surprise, the kinase had no constitutive activity nor dominant-negative properties, but it did retain sensitivity to WNK4 because NKCC1 activity was stimulated by coinjecting WNK4 with the SPAK [T243E; Δ(356–398)] mutant (Fig. 7). To ensure that an active WNK4 was responsible for the phosphorylation of this SPAK mutant, we coexpressed a catalytically inactive WNK4 (K183M) and demonstrated no cotransporter activation (Fig. 7). Because residue T243 was mutated into glutamic acid and S383 was absent in this mutant, it was likely that another residue was being phosphorylated by WNK4. Basophilic kinases phosphorylate serine/threonine residues preceded by basic residues at positions P-2 or P-5 (35). Close examination of the residues surrounding T243 and S383 revealed basic (positive) residues at positions P-2 or P-5, suggesting the possibility that WNK4 is a basophilic kinase. Another serine residue (S321), previously shown to be a target of PKC-θ phosphorylation (21), is preceded by an arginine at P-5 (see sequence *inset* in Fig. 7). To assess the role of S321 in the SPAK-NKCC regulatory pathway, we first mutated S321 into an alanine (S321A) in the wild-type kinase and found that it neither affected isotonic activation of NKCC1 nor prevented the activation of the cotransport when coexpressed with wild-type WNK4 (Fig. 7). Interestingly, combination of the S321A mutation with the activation loop T243E mutation resulted in a constitutively active SPAK that was capable of fully activating the cotransporter independent of upstream phosphorylation/activation by WNK4. However, introduction of the S321A mutation into the SPAK [T243E; Δ(356–398)] variant completely abrogated cotransporter activity both alone or when coexpressed with WNK4 (Fig. 7).

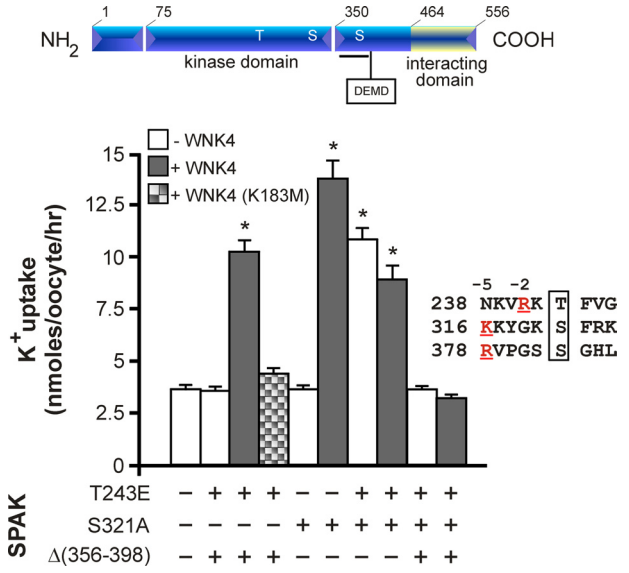

Fig. 7. Role of S321 in SPAK activation. *Top*: schematic representation of SPAK showing the position of the putative residues phosphorylated by WNK4. Horizontal line represents deleted segment (amino acid residues 356–398). Boxed residues (DEMD) represent a caspase cleavage site. *Bottom*: effect of deletion of a 43 amino acid fragment of the regulatory domain on SPAK activity. Kinase activity was assessed in *Xenopus laevis* oocytes through its ability to activate NKCC1 in the presence or absence of WNK4. NKCC1 activity was measured through $K^+(^{86}Rb^+)$ uptake under isosmotic conditions. *Inset*: sequence surrounding the S/T residues which are putative targets of WNK4 phosphorylation. Basic residues at positions P-2 and P-5 are colored red and underlined. Bars represent means ± SE of the flux (expressed in nanomoles per oocyte per hour; n = 20–25 oocytes). Each condition was tested at least twice with independent oocytes isolated from different frogs. *Significant ($P < 0.001$) difference between wild-type NKCC1 coexpressed with wild-type and mutant forms of SPAK.

DISCUSSION

Previous studies have identified the region of the cytosolic NH_2-terminal tail of NKCC1 which is phosphorylated upon cotransport activation (6, 14, 32). In the present study, we examined this region by site-directed mutagenesis to help identify the determinants of the kinase substrate recognition site. First, our experiments determined that the number of amino acid residues separating T206 and T211 is critical to SPAK substrate targeting. Reduction to three residues or insertion of a fifth residue between the two threonines completely disrupted NKCC1 function. Interestingly, this four-residue requirement was only true for T206 and T211, but not for T197 and T201 (which are separated by just three residues), nor T201 and T206, because removal of L204 did not affect NKCC1 function. These data suggest that the 206–211 pair constitutes the primary recognition site of the kinase, and that the distance between additional residues phosphorylated by SPAK is less stringent. The requirement for four residues for substrate recognition appears to be evolutionarily conserved because the two serines in the *Caenorhabiditis elegans* chloride channel CLH-3 which are phosphorylated by the *C. elegans* orthologue of mammalian OSR1 (germinal center kinase-3) are also separated by four amino acids (12).

Another requirement of the primary substrate recognition site seems to be the presence of a hydrophobic residue following T206. Although alanine substitution of the methionine residue immediately after T211 (M212A) had no effect on NKCC1 function, mutation of the phenylalanine (F207A) completely abrogated NKCC1 activity. Interestingly, the two serine residues (S474 and S479) targeted for phosphorylation in CLH-3 are also followed by hydrophobic residues isoleucine and phenylalanine, respectively (12). The presence of an hydrophobic residue following T206 is critical for proper positioning of the threonine. Indeed, many S/T protein kinases have a conserved hydrophobic pocket in the catalytic domain which accommodates hydrophobic amino acids and facilitates the placement of the targeted S/T in proximity to the Mg^{2+} and ATP binding sites. The hydrophobic pocket in mouse SPAK is lined by residues F244, P248, M251, and L294 (13).

Alignment of mouse and human NKCC and NCC sequences revealed the presence of conserved aspartic acid residues around the threonine region. Although positively charged residues are typically found in kinase consensus sequences, the presence/requirement of negatively charged residues has been also reported (19). Thousand and one amino acid kinase (TAO2), another Ste20 kinase, has an aspartic acid located at position P-5 which interacts with a positively charged pocket consisting of three positive residues (34). Mutation of these basic residues prevents substrate phosphorylation. We therefore mutated the two aspartic acids and found that a negative residue at position 213 was essential for cotransporter function. Indeed, mutation of this residue into alanine, but not glutamic acid, abrogated NKCC1 function. The position of this residue was also critical because it could not be moved to position 212. Whether this residue takes part in kinase substrate recognition or is a residue that is otherwise critical to NKCC1 function is unknown. Because of the predominant role of positively charged residues in kinase consensus sequences, the presence of an arginine residue at position 205 in mouse NKCC1 was also examined. This residue is conserved in NKCC1 and NCC, but not in NKCC2 (Fig. 1). Mutation of this positively charged residue to glutamine or asparagine (residues with amide side chains) or to alanine had little effect on NKCC1 activity, indicating that a basic residue is not required for kinase substrate recognition.

Mass spectrometry and Edman sequencing data revealed that WNK4 phosphorylates SPAK at residues T243 and S383 (32). On the basis of these data, we postulated that substitution of T243 and S383 into residues that mimic phosphorylation (aspartic acid or glutamic acid) should lead to kinase activation. We found that T243E (but not T243D) when combined with S383D rendered the kinase constitutively active. The role of T243 phosphorylation in SPAK activation was not unexpected because protein kinases undergo major rearrangements of the activation segment upon phosphorylation (25). Phosphorylation repositions the activation loop in such a way that it becomes compatible with substrate recognition and binding. We had previously shown that residues T243 and T247 in the activation loop were essential for kinase function and that both residues were phosphorylated in in vitro kinase reaction experiments (13). Our experiments here demonstrated that T243 phosphorylation requires WNK4 and therefore is not the result of kinase autophosphorylation. Indeed, we showed that the S383D mutant required the presence of WNK4 for activation. The role of residue T247 in the activation loop is less clear. While this residue is also phosphorylated, its mutation into a glutamic acid completely abrogated SPAK function (data not shown). Absence of function of a T247E mutant could be due

to the possible disruption of a dimer. Indeed, the crystal structure of the catalytic domain of OSR1 suggests that T247 (in SPAK) is located within an extended P + 1 loop domain that is exchanged or swapped between two SPAK monomers constituting an intertwined dimer (20).

The role of S383 phosphorylation in SPAK activation is also not fully understood. Because phosphorylation of S383 is also required for kinase activation, we assumed that mutation of S383 into an alanine would prevent activation. On the contrary, we found that S383A mutation behaved like wild-type SPAK, i.e., it activated K^+ uptake when co-injected with WNK4 and NKCC1 but was silent when co-injected with NKCC1 alone. Furthermore, S383A when combined with T243E also resulted in a constitutively active kinase. These data indicated that S383 was a critical residue which when mutated or phosphorylated led to kinase activation. In fact, our mutagenesis efforts revealed that S383 is part of a "larger domain" which participates in kinase activation. The structure of this domain and/or its interaction with other regions of the kinase likely defines whether or not the kinase is active or inactive. Autoinhibitory domains have been described for many protein kinases, including some mammalian Ste20 kinases (3, 4, 17, 24, 26, 33). Because all residues surrounding S383, when mutated, resulted in kinase activation, we postulate that the domain likely forms a weak interaction with another part of the kinase and that this interaction can be easily broken by subtle structural changes. The fact that all amino acids surrounding S383 are highly conserved in SPAK and OSR1 in multiple species is consistent with this idea. If the S383-containing domain inhibits SPAK through domain (protein-protein) interaction, it would constitute an autoinhibitory domain.

Because deletion of an autoinhibitory domain typically leads to increased kinase activity, we deleted amino acid segment 358–396 in the T243E SPAK mutant. We were surprised to see that the deletion did not result in an activated kinase, but in a kinase that still needed WNK4 activation. This was intriguing since T243 was mutated into a glutamic acid and S383 was absent. One possible explanation for this result is that there was another residue targeted by WNK4 which was masked by the presence of amino acids 358–396 and therefore previously unidentified. Deletion of this S383-containing segment thus "unmasked" a novel target of WNK4 phosphorylation. Close examination of the residues surrounding mouse SPAK T243 and S383 revealed the presence of basic residues located at positions P-2 or P-5, suggesting that WNK4 might be a basophilic kinase. In support of this possibility is the presence of a pair of acidic residues located in the major groove: D303 at the COOH terminus of the catalytic loop and E364 at the COOH-terminal end of helix αF. These negative residues have been shown to confer a strong preference for positive residues two or five positions upstream of the phospho-site in the target (35). On the basis of this information, we identified S321 as another possible target of WNK4 and showed that S321 participates in SPAK activation, because its mutation into an alanine in conjunction with T243E conferred constitutive activity. Furthermore, introduction of S321A into the (T243E; Δ358–396) mutant prevented WNK4 activation. Whether S321 is phosphorylated by WNK4 in wild-type SPAK and this phosphorylation was undetected by mass spectrometry (32) is still unresolved. Again, it is also possible that the deletion of 43 amino acids might have altered the tertiary structure of SPAK and thus allowed WNK4 to recognize S321 as a novel target. Interestingly, S321 was previously shown to be a target of PKC-θ phosphorylation (21). This finding, when combined with the observation that PKC-δ, another isotype of PKC, participates in the hypertonic stimulation of NKCC1 in human airway epithelial cells (29), suggests that not only WNK kinases stimulate SPAK/OSR1 by phosphorylation, but that other protein kinases might also modulate SPAK/OSR1 function through direct phosphorylation.

In summary, our studies have identified several key residues which contribute to the SPAK substrate recognition on the Na-K-2Cl cotransporter. We have also identified several phospho-residues in SPAK which participates in the activation the kinase and identified a region of the regulatory domain of the kinase which inhibits kinase activity. Evidence for multiple sites of kinase activation suggests the possibility of multiple signaling pathways converging to SPAK activation and phosphorylation of NKCC1.

ACKNOWLEDGMENTS

We thank Ghali Abdelmessih for help in the husbandry and surgery of the *Xenopus laevis* frogs, and Kerri Rios for technical assistance in creating some of the mutants and for preparing the DNA for transcription.

GRANTS

This work was supported by National Institutes of Health Grant GM074771 (to E. Delpire).

DISCLOSURES

No conflicts of interest, financial or otherwise, are declared by the authors.

REFERENCES

1. **Alvarez-Leefmans FJ, Gamiño SM, Giraldez F, Nogueron I.** Intracellular chloride regulation in amphibian dorsal root ganglion neurons studied with ion-selective microelectrodes. *J Physiol* 406: 225–246, 1988.
2. **Castrop H, Schnermann J.** Isoforms of renal Na-K-2Cl cotransporter NKCC2: expression and functional significance. *Am J Physiol Renal Physiol* 295: F859–F866, 2008.
3. **Ching YP, Leong VY, Wong CM, Kung HF.** Identification of an autoinhibitory domain of p21-activated protein kinase 5. *J Biol Chem* 278: 33621–33624, 2003.
4. **Creasy CL, Ambrose DM, Chernoff J.** The Ste20-like protein kinase, Mst1, dimerizes and contains an inhibitory domain. *J Biol Chem* 271: 21049–21053, 1996.
5. **Crouch JJ, Sakaguchi N, Lytle C, Schulte BA.** Immunohistochemical localization of the Na-K-Cl co-transporter (NKCC1) in the gerbil inner ear. *J Histochem Cytochem* 45: 773–778, 1997.
6. **Darman RB, Forbush B.** A regulatory locus of phosphorylation in the N terminus of the Na-K-Cl cotransporter, NKCC1. *J Biol Chem* 277: 37542–37550, 2002.
7. **Delpire E.** The mammalian family of sterile 20p-like protein kinases. *Pflügers Arch* 458: 953–967, 2009.
8. **Delpire E, Gagnon KB.** Genome-wide analysis of SPAK/OSR1 binding motifs. *Physiol Genomics* 28: 223–231, 2007.
9. **Delpire E, Lu J, England R, Dull C, Thorne T.** Deafness and imbalance associated with inactivation of the secretory Na-K-2Cl co-transporter. *Nat Genet* 22: 192–195, 1999.
10. **Delpire E, Rauchman MI, Beier DR, Hebert SC, Gullans SR.** Molecular cloning and chromosome localization of a putative basolateral Na-K-2Cl cotransporter from mouse inner medullary collecting duct (mIMCD-3) cells. *J Biol Chem* 269: 25677–25683, 1994.
11. **Edgcomb SP, Murphy KP.** Variability in the pKa of histidine side-chains correlates with burial within proteins. *Proteins* 49: 1–6, 2002.
12. **Falin RA, Morrison R, Ham AJ, Strange K.** Identification of regulatory phosphorylation sites in a cell volume- and Ste20 kinase-dependent ClC anion channel. *J Gen Physiol* 133: 29–42, 2009.

13. **Gagnon KB, England R, Delpire E.** Characterization of SPAK and OSR1, regulatory kinases of the Na-K-2Cl cotransporter. *Mol Cell Biol* 26: 689–698, 2006.
14. **Gagnon KB, England R, Delpire E.** A single binding motif is required for SPAK activation of the Na-K-2Cl cotransporter. *Cell Physiol Biochem* 20: 131–142, 2007.
15. **Gagnon KB, England R, Delpire E.** Volume sensitivity of cation-chloride cotransporters is modulated by the interaction of two kinases: SPAK and WNK4. *Am J Physiol Cell Physiol* 290: C134–C142, 2006.
16. **Gimenez I, Forbush B.** Regulatory phosphorylation sites in the NH_2 terminus of the renal Na-K-Cl cotransporter (NKCC2). *Am J Physiol Renal Physiol* 289: F1341–F1345, 2005.
17. **Glantschnig H, Rodan GA, Reszka AA.** Mapping of MST1 kinase sites of phosphorylation. Activation and autophosphorylation. *J Biol Chem* 277: 42987–42996, 2002.
18. **Greger R.** Ion transport mechanisms in thick ascending limb of Henle's loop of mammalian nephron. *Physiol Rev* 65: 760–797, 1985.
19. **Kennelly PJ, Krebs EG.** Consensus sequences as substrate specificity determinants for protein kinases and protein phosphatases. *J Biol Chem* 266: 15555–15558, 1991.
20. **Lee SJ, Cobb MH, Goldsmith EJ.** Crystal structure of domain-swapped STE20 OSR1 kinase domain. *Protein Sci* 18: 304–313, 2009.
21. **Li Y, Hu J, Vita R, Sun B, Tabata H, Altman A.** SPAK kinase is a substrate and target of PKCtheta in T-cell receptor-induced AP-1 activation pathway. *EMBO J* 23: 1112–1122, 2004.
22. **Liedtke CM.** Regulation of chloride transport in epithelia. *Annu Rev Physiol* 51: 143–160, 1989.
23. **Moriguchi T, Urushiyama S, Hisamoto N, Iemura SI, Uchida S, Natsume T, Matsumoto K, Shibuya H.** WNK1 regulates phosphorylation of cation-chloride-coupled cotransporters via the STE20-related kinases, SPAK and OSR1. *J Biol Chem* 280: 42685–42693, 2006.
24. **Mukherji S, Brickey DA, Soderling TR.** Mutational analysis of secondary structure in the autoinhibitory and autophosphorylation domains of calmodulin kinase II. *J Biol Chem* 269: 20733–20738, 1994.
25. **Nolen B, Taylor S, Ghosh G.** Regulation of protein kinases: controlling activity through activation segment conformation. *Mol Cell* 15: 661–675, 2004.
26. **Pang T, Xiong B, Li JY, Qiu BY, Jin GZ, Shen JK, Li J.** Conserved alpha-helix acts as autoinhibitory sequence in AMP-activated protein kinase alpha subunits. *J Biol Chem* 282: 495–506, 2007.
27. **Piechotta K, Garbarini NJ, England R, Delpire E.** Characterization of the interaction of the stress kinase SPAK with the Na^+-K^+-$2Cl^-$ cotransporter in the nervous system: evidence for a scaffolding role of the kinase. *J Biol Chem* 278: 52848–52856, 2003.
28. **Piechotta K, Lu J, Delpire E.** Cation-chloride cotransporters interact with the stress-related kinases SPAK and OSR1. *J Biol Chem* 277: 50812–50819, 2002.
29. **Smith L, Smallwood N, Altman A, Liedtke CM.** PKCdelta acts upstream of SPAK in the activation of NKCC1 by hyperosmotic stress in human airway epithelial cells. *J Biol Chem* 283: 22147–22156, 2008.
30. **Sung KW, Kirby M, McDonald MP, Lovinger DM, Delpire E.** Abnormal $GABA_A$-receptor mediated currents in dorsal root ganglion neurons isolated from Na-K-2Cl cotransporter null mice. *J Neurosci* 20: 7531–7538, 2000.
31. **Villa F, Goebel J, Rafiqi FH, Deak M, Thastrup J, Alessi DR, van Aalten DMF.** Structural insights into the recognition of substrates and activators by the OSR1 kinase. *EMBO Rep* 8: 839–845, 2007.
32. **Vitari AC, Deak M, Morrice NA, Alessi DR.** The WNK1 and WNK4 protein kinases that are mutated in Gordon's hypertension syndrome, phosphorylate and active SPAK and OSR1 protein kinases. *Biochem J* 391: 17–24, 2005.
33. **Zhao ZS, Manser E, Chen XQ, Chong C, Leung T, Lim L.** A conserved negative regulatory region in alphaPAK: inhibition of PAK kinases reveals their morphological roles downstream of Cdc42 and Rac1. *Mol Cell Biol* 18: 2153–2163, 1998.
34. **Zhou T, Raman M, Gao Y, Earnest SC, Z, Machius M, Cobb MH, Goldsmith EJ.** Crystal structure of the TAO2 kinase domain: activation and specificity of a Ste20p MAP3K. *Structure* 12: 1891–1900, 2004.
35. **Zhu G, Fujii K, Liu Y, Codrea V, Herrero J, Shaw S.** A single pair of acidic residues in the kinase major groove mediates strong substrate preference for P-2 or P-5 arginine in the AGC, CAMK, and STE kinase families. *J Biol Chem* 280: 36372–36379, 2005.